Current Trends in Biotechnology and Pharmacy
Vol. 19 (Supplementary Issue 4), Oct-Dec 2025, ISSN 0973-8916 (Print)., 2230-7303 (Online)
10.5530/ctbp.2025.4s.4

In Silico Elucidation of Antineoplastic Mechanisms in *Cucurbita pepo* Seed Extract Using Advanced Molecular Modeling Techniques

V.Prisicilla Pushparani[1]*, K.S.Nithin Sai[2], and T. P. Rajarajan[3]

[1]Department of Bioengineering, Institute of Biotechnology, Saveetha School of Engineering, Saveetha Institute of Medical and Technical Sciences, Thandalam, Chennai-602 105, Tamil Nadu, India
[2] Institute of Biological Sciences, Faculty of Science, Universiti Malaya, 50603 Kuala Lumpur, Malaysia
[3]Department of Biotechnology, St. Peter's College of Engineering and Technology, Avadi, Chennai-600 054, Tamil Nadu, India
Corresponding author: priscillapushparaniv.sse@saveetha.com

Abstract

Cancer continues to pose a significant global health burden, with lung and breast cancer among the most frequently diagnosed types. In this study, the most nutrition-rich andanticancer potential of *Cucurbita pepo* (pumpkin) seed extract was investigated using an integrative computational biology approach. Bioactive constituents from the aqueous extract were identified through Gas Chromatography-Mass Spectrometry (GC-MS) analysis. Molecular docking studies, conducted using PyRx, evaluated the binding affinity of these phytochemicals toward the HER2 (PDB ID: 3PP0) receptor, a critical target in cancer therapeutics. Notably, Stearic acid glycidyl ester, Linoleic acid, and Trilinolein demonstrated strong binding interactions with HER2, suggesting their role in modulating oncogenic pathways.

Drug-likeness and pharmacokinetic parameters were assessed via ADMET analysis, confirming favorable bioavailability and toxicity profiles. The most promising compound-receptor complex was further validated through a 100-nanosecond molecular dynamics simulation, which revealed sustained structural stability. These findings propose *C. pepo* as a promising natural source of anticancer agents andprovide a strong basis for future in-vitro and in-vivo experimental validation.

Keywords: *Cucurbita pepo*, HER2, Cancer, Phytochemicals,Nutrition, Molecular Docking and Simulation

1. Introduction

Cancer exists as the most prevalent, life-threatening and detrimental disease in the current generation, affecting individuals globally with no specific age limit (1). Among various cancer types, lung cancer and breast cancer are two of the leading causes of mortality (related to cancer) worldwide (2). Lung cancer is often associated with tobacco smoke and environmental pollution and shows a high incidence for both active and passive smokers (3). Symptoms for lung cancer typically appear at advanced stages (stage III and IV) and include hemoptysis, chest pain, hoarseness, dyspnea, anorexia, and facial swelling. Breast cancer, on the other hand, arises due to the formation of breast epithelial cells such as palpable masses, mutations, morphological breast changes, and axillary lymphadenopathy (4). Women over the age of 35 are being predominantly affected by breast cancer and is influenced by genetic factors, notably mutations in BRCA1 and BRCA2 genes, as well as hormonal imbalances (5). Pathogenesis of breast cancer involves deregulated gene expression of adhesion molecules E-cadherin, catenins, etc., which are characteristics of invasive lobular carcinoma due to their major involvement in mammary gland development and tumor progression(6).

Diagnostic approaches for breast and lung cancer include mammography, MRI, CT scan, etc., offering enhanced sensitivity in specific populations with standard treatments such as surgical resection, chemotherapy and

Vol. 19 (Supplementary Issue 4), Oct-Dec 2025, ISSN 0973-8916 (Print)., 2230-7303 (Online)
10.5530/ctbp.2025.4s.4

radiotherapy, targeted therapies for advanced stages are utilized effectively. However, despite such advancements, cancer continues to pose a major public health challenge with a five-year survival rate of 20 - 30%, largely due to late-stage diagnosis, treatment of side effects, and aggressive disease progression (7).

HER2 (human epidermal growth factor receptor 2) is a membrane-bound tyrosine kinase which is encoded by the ERBB2 gene and plays a crucial role in cell proliferation and survival. Overexpression of HER2 genes is a key factor and occurs in 15 - 20% of breast cancer cases, making it a key therapeutic target (8). In addition, certain HER2 mutations hold clinical relevance in non-small cell lung cancer (NSCLC) by favoring tumor progression. Though cancer heterogeneity can cause discrepancies, HER2 status assessment using immunohistochemistry (IHC) and in situ hybridization (ISH) is widely considered as essential and development of newer assays like the gene-protein assay (GPA) improve diagnostic precision (9, 10). Inspite of having such remarkable advancements, standardized treatment protocols and therapies are still under development, and understanding HER2 biology can aid in enhancing the process of developing refined detection methods and modulate cancer progression and help patients recover with minimal to no side effects (11).

Recently, the interest in plant-based nutraceuticals is being focused on their easy availability, natural profile, presence of diverse bioactive compounds and wide range of therapeutic and pharmacological effects (12). Being native to North America and widely cultivated for both culinary and medicinal uses, seeds of *Cucurbita pepo* (Pumpkin) are rich in dietary fiber, polyunsaturated fatty acids, magnesium, iron, carotenoids, and antioxidants. In particular, their carotenoids are associated with free radical-scavenging properties, providing evident anti-oxidant profile and underscoring the urge to explore their potential in mitigating cancer (13).A robust systematic *in-silico* validation of the compounds identified from GC-MS analysis of *Cucurbita pepo seeds was* performed with molecular docking, ADMET evaluation and Molecular Dynamic Simulations, offering detailed insights on how the bioactive compounds interact with the protein HER2. The study aims to identify the best drug candidatesfromnutrition-rich pumpkin seedderived phytochemicals and laying foundation for future in vivo studies and drug development.

2. Methods and Materials:

2.1. Collection & preparation of plant material

The seeds are uprooted from freshly obtained *Cucurbita pepo* stored in room temperature to avoid moisture formation. The seeds were cleaned, blended to powder under dry conditions and stored in an airtight labelled container (14)

2.2. SoxhletExtraction:

25g of the powdered seeds are packed in filter paper (20x20 cm) folded cylindrical vise and packed to avoid wastage. This is introduced to a sterilized Soxhlet's round bottom flask, which was then filled with 250ml of distilled water and headed at 90℃. 21 cycles were allowed as standard, and the extract was dried,frozen after extraction and stored in an air-tight container (14).

2.3.Gas Chromatography-Mass Spectrometry (GC–MS) analysis:

The aqueous extract was characterized using Fisons MD 800 single quadrupole detector GC-MS system. The setup was encased in a heated and thermocouple containingan outer tube, with a 28 V DC spiral heater power supply. Insulated stainless steel vacuum housing was provided, and electron impact ionization (EI) at 70 eV was used as the standard ionization method. As temperature rose to 280 °C, EI provides universal ionization and efficient fragmentation, allowing us to identify organic compounds via the detector (15).

Vol. 19 (Supplementary Issue 4), Oct-Dec 2025, ISSN 0973-8916 (Print)., 2230-7303 (Online)
10.5530/ctbp.2025.4s.4

2.4. Molecular Docking Studies

2.4.1 Protein and Ligand Structure Preparation

The ligands from GC-Ms were downloaded as SDF file format structures from PubChem Database. To these compounds, energy minimization was performed, and the structures were converted to PDBQT format using PyRx(16).

Crystal Structure of the Kinase domain of Human HER2 (PDB ID: 3PP0) was obtained from RCSB PDB Data Base (PDB). This structure was processed by removing water molecules and unnecessary ligands using Pymol, and chain A was chosen for further*in-silico* analysis as it contains complete HER2 kinase domain (residues 703–1029) that is responsible for the protein's enzymatic activity (17). This protein file is added as macromolecule in PyRx and converted to its PDBQT format for docking analysis.

2.4.2. Molecular Docking Analysis

Molecular Docking was carried out for the 3D macromolecule and ligand structures using local server of Vina in PyRx (16). A grid box with the maximum size having dimensions X = 59.5691, Y = 48.1705 and Z = 59.0717 was set to cover the entire protein binding pockets, and the docked complexes were evaluated based on binding affinities. Optimal docking and stable complex is characterized by lower binding affinities and the interactions between the protein and the ligands were assessed using Ligplot evaluate involvement of active site residues (18).

2.5. Prediction of ADMET Properties

The drug-likeness, pharmacokinetic and Toxicity of the aqueous extract bioactive compounds were predicted using ADMET lab 2.0 and SwissADME online tool. In-*silico* ADMET screening is essential for assessing drug-likeness, metabolic stability, and toxicity risks at early-stage drug development. Parameters such as Lipinski's rule of 5, oral bioavailability, cytochrome P450 interactions, blood-brain barrier permeability and toxicological endpoints were carefully analyzed to identify most promising drug candidates (19)

2.6. Molecular Simulation Studies

Schrodinger LLC's Desmond program was used to examine the MD simulation over a 100ns run to study ligand-binding in a physiochemical environment (20). With Maestro protein preparation, the ligand complex was preprocessed to eliminate steric conflicts, deformation geometry, and poor contacts, while performing optimization and energy minimization to the complex (21). The model was constructed through system builder, orthorhombic shape, TIP3P model of solvent and OPLS-2005 force field. The model was then neutralized with counter ions sodium chloride 0.15 M, 300k temperature with 1 atm pressure and trajectory was saved after every 100ps (22). Using VSGB model, rotamer techniques and force OPLS-2005, the binding energy were determined following the execution of MD trajectory (shown in equation 1).

$$DGbind = Gcomplex - (Gprotein + Gligand) \quad (1)$$

3. Results and Discussion

The GC-MS profiling of the aqueous extract revealed 13 unique bioactive compounds characterized in (Table 1 and Fig. 1) based on the retention time, PubChem ID, Molecular Formula, Smiles annotation, and 2D structure.

The compounds reveal specific therapeutic relevance due to the presence of volatile aromatics, sulfur-containing metabolites, and ketones. Fatty acid derivatives such as linoleic acid and lipid esters have potential membrane penetration and drug delivery properties, while certain ketones and hydrocarbons are reported for their anticancer and antimicrobial activities. Bicyclic and ether-based compounds propose structural diversity in compounds for targeting HER2 protein and evaluating their role as anticancer agents.

Vol. 19 (Supplementary Issue 4), Oct-Dec 2025, ISSN 0973-8916 (Print)., 2230-7303 (Online)
10.5530/ctbp.2025.4s.4

Table 1: GC-MS Profile of Bioactive Compounds Identified in the Aqueous Extract of *C. pepo seeds*

S. No	Compound Name	Molecular Formula	PubChem ID	SMILES	2D Structure
1	BENZENE, ETHYL-	C_8H_{10}	7500	CCC1=CC=CC=C1	
2	BENZENE, 1,2-DIMETHYL-	C_8H_{10}	7237	CC1=CC=CC=C1C	
3	2-PENTANETHIOL, 2-METHYL-	$C_6H_{14}S$	74213	CCCC(C)(C)S	
4	3-NONANONE	$C_9H_{18}O$	61235	CCCCCCC(=O)CC	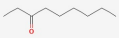
5	Pentane, 3-ethyl-2,4-dimethyl-	C_9H_{20}	14040	CCC(C(C)C)C(C)C	
6	3-HEXEN-2-ONE	$C_6H_{10}O$	5367744	CC/C=C/C(=O)C	
7	9,12-Octadecadienoic acid (Z,Z)-	$C_{18}H_{32}O_2$	5280450	CCCCC/C=C\C/C=C\CCCCCCC(=O)O	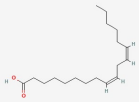
8	9-Octadecenoic acid, 1,2,3-propanetriyl ester, (E,E,E)-	$C_{57}H_{104}O_6$	5364673	CCCCCCCC/C=C/CCCCCCCC(=O)OCC(OC(=O)CCCCCCC/C=C/CCCCCCCC)COC(=O)CCCCCCC/C=C/CCCCCCCC	
9	HEXADECANOIC ACID, 2-HYDROXY-1,3-PROPANEDIYL ESTER	$C_{35}H_{68}O_5$	68149	CCCCCCCCCCCCCCCC(=O)OCC(COC(=O)CCCCCCCCCCCCCC)O	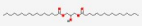

Vol. 19 (Supplementary Issue 4), Oct-Dec 2025, ISSN 0973-8916 (Print)., 2230-7303 (Online)
10.5530/ctbp.2025.4s.4

10	Bicyclo[10.1.0]tridec-1-ene	$C_{13}H_{22}$	548879	C1CCCCC=C2CC2CCCC1	
11	Glycidol stearate	$C_{21}H_{40}O_3$	62642	CCCCCCCCCCCCCCCCCC(=O)OCC1CO1	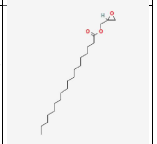
12	DODECANOIC ACID, 1,2,3-PROPANETRIYL ESTER	$C_{39}H_{74}O_6$	10851	CCCCCCCCCCCC(=O)OCC(COC(=O)CCCCCCCCCCC)OC(=O)CCCCCCCCCCCC	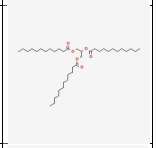
13	Lauric acid, 2-(hexadecyloxy)-3-(octadecyloxy) propyl ester	$C_{49}H_{98}O_4$	635296	CCCCCCCCCCCCCCCCCCC-OCC(COC(=O)CCCCCCCCCCCC)OCCCCCCCCCCCCCCCCC	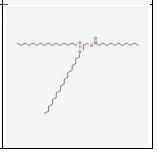

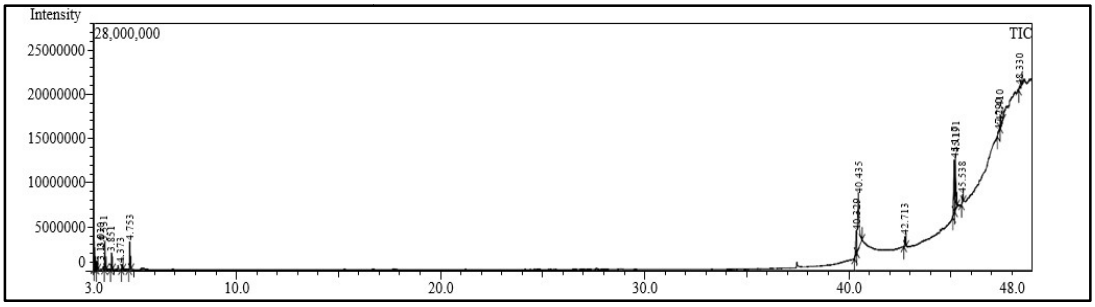

Fig. 1: GC–MS Chromatogram of *C. pepo* Seed Aqueous Extract Showing Retention Time of the Identified Bioactive Phytocompounds

3.1. Molecular Docking Analysis

Docking analysis evaluated the binding affinities of the bioactive compounds against HER2 protein, and the results show several candidates with promising interactions with the protein.Ligplot results of the top 4 ligands were assessed to check if their binding wasfavored for active site residues which could potentially inhibit the protein activity or disrupt its stability (Table 2 and Fig. 2). Compound 9,12-octadecadienoic acid (Z, Z) showed the highest binding affinity of –6.3 kcal/malforming hydrogen bonds with key active site residues Thr798, Leu796 and Lys753, and hydrophobic contacts with Val734, Leu852 and Ala751 which are stabilizing ligands within HER2's ATP-binding pocket (17). Following this, lauric acid, 2-(hexadecyloxy)-3-(octadecyloxy)propyl ester appeared as the second-best compound having–6.2kcal/mol and showed hydrogen bonding with Asp863 and Arg849, with numerous van der Waals interactions favoring strong anchoring and membrane penetration.

Glycidol stearate and Bicyclo[10.1.0] tridec-1-ene both had binding affinities of -6.1 kcal/mol. Glycidol stearate had no hydrogen

Vol. 19 (Supplementary Issue 4), Oct-Dec 2025, ISSN 0973-8916 (Print)., 2230-7303 (Online)
10.5530/ctbp.2025.4s.4

Table 2: Binding Affinities of Bioactive Compounds Identified from C. pepo seed extracts against HER2 protein

Compound Name	Binding Affinity (kcal/mol)	No. of Interacting Residues
9,12-Octadecadienoic acid (Z,Z)-	-6.3	7
Lauric acid, 2-(hexadecyloxy)-3-(octadecyloxy)propyl ester	-6.2	7
Bicyclo[10.1.0]tridec-1-ene	-6.1	6
Glycidol stearate	-6.1	6
BENZENE, 1,2-DIMETHYL-	-5.7	7
BENZENE, ETHYL-	-5.5	5
Pentane, 3-ethyl-2,4-dimethyl-	-5.3	11
HEXADECANOIC ACID, 2-HYDROXY-1,3-PROPANEDIYL ESTER	-5.3	15
3-NONANONE	-5.1	12
9-Octadecenoic acid, 1,2,3-propanetriyl ester, (E,E,E)-	-5.1	7
DODECANOIC ACID, 1,2,3-PROPANETRIYL ESTER	-5.1	18
3-HEXEN-2-ONE	-4.6	15
2-PENTANETHIOL, 2-METHYL-	-4.1	27

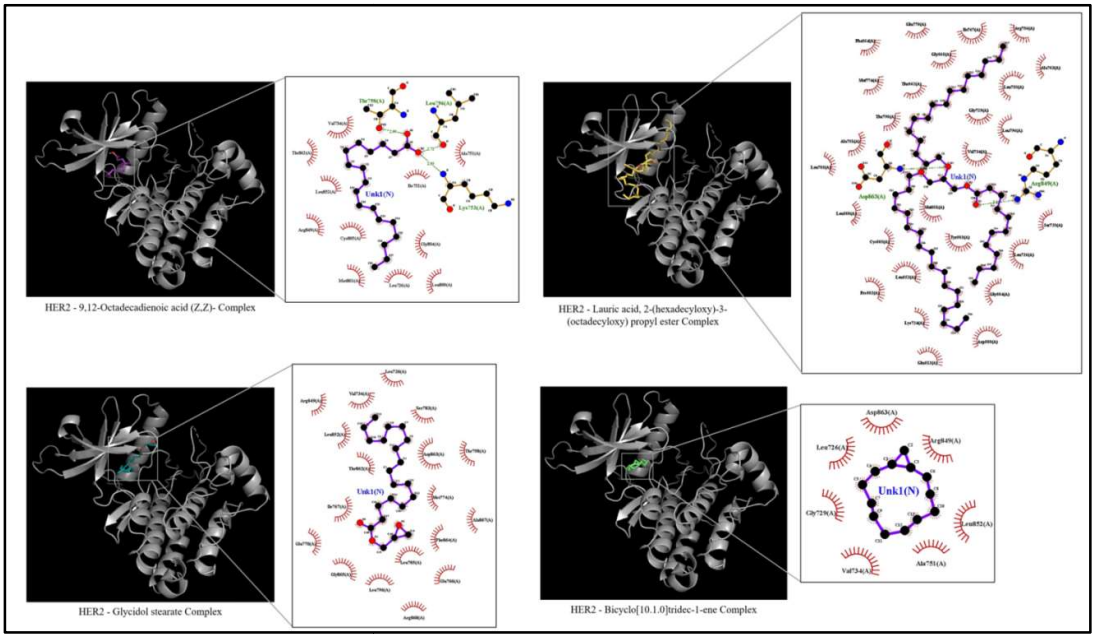

Fig. 2: Molecular Docking and Interaction Plots of C. pepo Seed Extract Compounds with HER2 Protein

In Silico Elucidation of Antineoplastic Mechanisms

Vol. 19 (Supplementary Issue 4), Oct-Dec 2025, ISSN 0973-8916 (Print)., 2230-7303 (Online)
10.5530/ctbp.2025.4s.4

Table 3: Physicochemical Evaluation of Bioactive Compounds Identified from Aqueous Extract of *C. pepo* seeds

Compound Name	Molecular Weight (g/mol)	Heavy Atoms	Aromatic Heavy Atoms	Fraction Csp^3	Rotatable Bonds	H-bond Acceptors	H-bond Donors	Molar Refractivity	TPSA ($Å^2$)
BENZENE, ETHYL-	106.17	8	6	0.25	1	0	0	36.22	0
BENZENE, 1,2-DIMETHYL-	106.17	8	6	0.25	0	0	0	36.37	0
2-PENTANETHIOL, 2-METHYL-	118.24	7	0	1	2	0	0	38.92	38.8
3-NONANONE	142.24	10	0	0.89	6	1	0	45.58	17.07
Pentane, 3-ethyl-2,4-dimethyl-	128.26	9	0	1	3	0	0	45.38	0
3-HEXEN-2-ONE	98.14	7	0	0.5	2	1	0	30.68	17.07
9,12-Octadecadienoic acid (Z,Z)-	280.45	20	0	0.72	14	2	1	89.46	37.3
9-Octadecenoic acid, 1,2,3-propanetriyl ester, (E,E,E)-	885.43	63	0	0.84	53	6	0	278.55	78.9
HEXADECANOIC ACID, 2-HYDROXY-1,3-PROPANEDIYL ESTER	568.91	40	0	0.94	34	5	1	174.09	72.83
Bicyclo[10.1.0]tridec-1-ene	178.31	13	0	0.85	0	0	0	59.9	0
Glycidol stearate	340.54	24	0	0.95	19	3	0	103.32	38.83
DODECANOIC ACID, 1,2,3-PROPANETRIYL ESTER	639	45	0	0.92	38	6	0	193.44	78.9
Lauric acid, 2-(hexadecyloxy)-3-(octadecyloxy)propyl ester	751.3	53	0	0.98	48	4	0	241.11	44.76

bonds but formed hydrophobic interactions with a dense network of residues such as Met774, Thr798, Leu785 and Phe864, while Bicyclo[10.1.0] tridec-1-ene also had consistent hydrophobic contact with residues like Val734, Ala751 and Leu852. These interactions and the long fatty acid or complex ester chains of the compounds suggest that their structures possess enhanced lipophilic interactions and membrane permeability, which is crucial for targeting HER2, a transmembrane protein (23). Compounds such as 2-pentanethiol, 2-methyl- and 3-hexen-2-one showed lower binding affinities suggesting that they may possess comparatively weaker interactions. The results suggest that lipid or ester-based compounds may offer better binding and has potential to modulate HER2 protein function.

3.2. ADMET Characterization

3.2.1. Analysis of Physicochemical Properties

The aqueous extract compounds showed diverse physicochemical characteristics such as molecular weight, polarity, hydrogen bonding potential, etc., serving as a critical factor for evaluating their pharmacological behavior against HER2 protein (Table 3).

Vol. 19 (Supplementary Issue 4), Oct-Dec 2025, ISSN 0973-8916 (Print)., 2230-7303 (Online)
10.5530/ctbp.2025.4s.4

Table 4: Pharmacokinetic and Drug-Likeness Analysis of Ligands identified from aqueous *C. pepo* Extracts using SwissADME

Parameter	GI Absorption	BBB Permeant	P-gp Substrate	CYP Inhibitor					Log Kp (Skin Permeation)	Lipinski Rule	Bioavailability Score
				CYP1A2	CYP2C19	CYP2C9	CYP2D6	CYP3A4			
BENZENE, ETHYL-	Low	No	No	No	No	No	No	No	-4.71 cm/s	Yes; 0 violations	0.55
BENZENE, 1,2-DIMETHYL-	Low	Yes	No	No	No	No	No	No	-4.73 cm/s	Yes; 0 violations	0.55
2-PENTANETHIOL, 2-METHYL-	High	Yes	No	No	No	No	No	No	-5.33 cm/s	Yes; 0 violations	0.55
3-NONANONE	High	Yes	No	No	No	No	No	No	-5.15 cm/s	Yes; 0 violation	0.55
Pentane, 3-ethyl-2,4-dimethyl-	Low	Yes	No	No	No	No	No	No	-4.09 cm/s	Yes; 1 violation	0.55
3-HEXEN-2-ONE	High	Yes	No	No	No	No	No	No	-6.05 cm/s	Yes; 0 violation	0.55
9,12-Octadecadienoic acid (Z,Z)-	High	Yes	No	No	No	No	No	No	-6.05 cm/s	Yes; 0 violation	0.55
9-Octadecenoic acid, 1,2,3-propanetriyl ester, (E,E,E)-	Low	No	Yes	No	No	No	No	No	4.20 cm/s	No (2 violations: MW>500, MLOGP>4.15)	0.17
HEXADECANOIC ACID, 2-HYDROXY-1,3-PROPANEDIYL ESTER	Low	No	Yes	No	No	No	No	No	0.20 cm/s	No (2 violations: MW>500, MLOGP>4.15)	0.17
Bicyclo[10.1.0]tridec-1-ene	Low	No	No	No	No	Yes	No	No	-3.77 cm/s	Yes (1 violation: MLOGP>4.15)	0.55
Glycidol stearate	High	No	No	Yes	No	No	No	No	-2.49 cm/s	Yes (0 violations)	0.55

Vol. 19 (Supplementary Issue 4), Oct-Dec 2025, ISSN 0973-8916 (Print)., 2230-7303 (Online)
10.5530/ctbp.2025.4s.4

DODECANOIC ACID, 1,2,3-PROPANETRIYL ESTER	Low	No	Yes	No	No	No	No	No	0.76 cm/s	No (2 violations: MW > 500, MLOGP > 4.15)	0.17
Lauric acid, 2-(hexadecyloxy)-3-(octadecyloxy)propyl ester	Low	No	Yes	No	No	No	No	No	4.47 cm/s	No (2 violations: MW > 500, MLOGP > 4.15)	0.17

The molecular weight of the compounds ranged from as low as 98.14 g/mol for 3-HEXEN-2-ONE all the way up to 885.43 g/mol for 9-Octadecenoic acid, 1,2,3-propanetriyl ester, (E,E,E)-. Most of the high molecular weight compounds have esters or long fatty acid chains, especially 9,12-Octadecadienoic acid (Z,Z)-, Lauric acid derivatives and Glycidol stearate have anti-inflammatory and bioactive nature. Aromatic heavy atom counts in benzene derivatives indicate possible π-π stacking interactions while high molecular weight compounds have higher heavy atoms. Fraction Csp^3 levels were evaluated to analyze the solubility and stability of the compounds. High Csp^3 fractions having compounds such as Glycidol stearate, Lauric acid ester have improved metabolic stability and solubility (24).

Lipid esters showed more rotatable bonds,indicating their molecular flexibility for oral bioavailability and membrane permeability. In addition to this, esters 9-Octadecenoic acid, 1,2,3-propanetriyl ester, (E,E,E)-, HEXADECANOIC ACID, 2-HYDROXY-1,3-PROPANEDIYL ESTER and DODECANOIC ACID, 1,2,3-PROPANETRIYL ESTER had the highest hydrogen bond donor and acceptor count, and molar refractivity, thereby indicating their strong polarizability and solubility. TPSA values more than 70 $Å^2$ may possibly restrict blood–brain barrier penetration but allows drugs to cross membranes and target peripheral organs (25). These diverse compounds reflect the unexplored potential of C. pepo seeds, with compounds 9,12-Octadecadienoic acid (Z,Z)-, HEXADECANOIC ACID esters and Glycidol stearate standing out due to their favorable physicochemical properties.

3.2.2. Evaluation of Pharmacokinetic Properties

Drug-likeness and pharmacokinetic analysis of the bioactive compounds were carried out through a comprehensive *in-silico* ADME analysis. Key parameters such as gastrointestinal (GI) absorption, blood-brain barrier (BBB) permeability, P-glycoprotein (P-gp) substrate identification, cytochrome P450 (CYP) inhibition, skin permeation potential (Log Kp), Lipinski's rule of five compliance and overall bioavailability score are assessed (Table 4).

Compounds like 2-pentanethiol, 2-methyl-, 3-hexen-2-one, and 9,12-octadecadienoic acid (Z,Z) showed high GI absorption with 0 Lipinski violations and good skin permeability (Log Kp: -6.05 cm/s) making them the best candidates with strong oral and transdermal potential. On the other hand, 9-octadecenoic acid, 1,2,3-propanetriyl ester, hexadecenoic acid, 2-hydroxy-1,3-propanediyl ester, and lauric acid, 2-(hexadecyloxy)-3-(octadecyloxy)propyl ester had low GI absorption and multiple Lipinski violations limiting their oral bioavailability and increase the risk of off-target effects (26). P-gp Substrate inhibition was observed for 9-Octadecenoic acid, 1,2,3-propanetriyl ester, Hexadecanoic acid, 2-hydroxy-1,3-propanediyl ester and Dodecanoicacid,

Vol. 19 (Supplementary Issue 4), Oct-Dec 2025, ISSN 0973-8916 (Print)., 2230-7303 (Online)
10.5530/ctbp.2025.4s.4

Table 5: *In-silico*Prediction of Organ toxicity and Systemic Toxicological endpoints of selected *C. pepo* bioactive compounds

Compound Name	LD50 (mg/kg)	Toxicity Class	Organ Toxicity					Toxicity End Points			
			Hepatotoxicity	Neurotoxicity	Nephrotoxicity	Respiratory toxicity	Cardiotoxicity	Carcinogenicity	Immunotoxicity	Mutagenicity	Cytotoxicity
Benzene, ethyl-	810	4	Inactive (0.86)	Active (0.58)	Inactive (0.84)	Inactive (0.87)	Inactive (0.65)	Active (0.89)	Inactive (0.99)	Inactive (0.98)	Inactive (0.91)
Benzene, 1,2-dimethyl-	3567	5	Inactive (0.89)	Active (0.76)	Inactive (0.85)	Inactive (0.99)	Inactive (0.86)	Active (0.79)	Inactive (0.99)	Inactive (0.94)	Inactive (0.88)
2-Pentanethiol, 2-methyl-	1500	4	Inactive (0.81)	Inactive (0.68)	Inactive (0.88)	Active (0.69)	Inactive (0.85)	Inactive (0.68)	Inactive (0.99)	Inactive (0.92)	Inactive (0.77)
3-Nonanone	5000	5	Inactive (0.69)	Inactive (0.66)	Inactive (0.81)	Inactive (0.99)	Inactive (0.99)	Inactive (0.63)	Inactive (0.99)	Inactive (0.97)	Inactive (0.73)
Pentane, 3-ethyl-2,4-dimethyl-	2000	4	Inactive (0.90)	Inactive (0.57)	Inactive (0.85)	Active (0.98)	Inactive (0.76)	Inactive (0.59)	Inactive (0.99)	Inactive (0.97)	Inactive (0.79)
3-Hexen-2-one	3200	5	Inactive (0.82)	Inactive (0.56)	Inactive (0.77)	Inactive (0.83)	Inactive (0.52)	Active (0.57)	Inactive (0.99)	Inactive (0.77)	Inactive (0.80)
9,12-Octadecadienoic acid (Z,Z)-	10000	6	Inactive (0.55)	Inactive (0.91)	Inactive (0.55)	Inactive (0.84)	Inactive (0.99)	Inactive (0.64)	Inactive (0.96)	Inactive (1.00)	Inactive (0.71)
9-Octadecenoic acid, 1,2,3-propanetriyl ester (E,E,E)-	3520	5	Inactive (0.88)	Inactive (0.92)	Inactive (0.50)	Inactive (0.97)	Inactive (0.97)	Active (0.70)	Inactive (0.95)	Active (0.57)	Inactive (0.86)
Hexadecanoic acid, 2-hydroxy-1,3-propanediyl ester	5000	5	Inactive (0.89)	Inactive (0.94)	Active (0.56)	Inactive (0.82)	Inactive (0.96)	Active (0.56)	Inactive (0.98)	Inactive (0.61)	Inactive (0.85)
Bicyclo[10.1.0]tridec-1-ene	5000	5	Inactive (0.74)	Active (0.59)	Inactive (0.84)	Inactive (0.58)	Inactive (0.71)	Active (0.60)	Inactive (0.99)	Inactive (0.61)	Inactive (0.73)
Glycidol	100	6	Inactive	Inactive	Inactive	Inactiv	Inactive	Active	Inactive	Active	Inactiv

Vol. 19 (Supplementary Issue 4), Oct-Dec 2025, ISSN 0973-8916 (Print)., 2230-7303 (Online)
10.5530/ctbp.2025.4s.4

stearate	00		(0.85)	(0.86)	(0.52)	e (0.89)	(0.75)	(0.62)	(0.97)	(0.56)	e (0.79)
Dodecanoic acid, 1,2,3-propanetriyl ester	500 0	5	Inactive (0.88)	Inactive (0.92)	Inactive (0.50)	Inactiv e (0.98)	Inactive (0.93)	Active (0.74)	Inactive (0.98)	Active (0.68)	Inactiv e (0.86)
Lauric acid, 2-(hexadecylo xy)-3-(octadecylox y) propyl ester	500 0	5	Inactive (0.90)	Inactive (0.90)	Inactive (0.51)	Inactiv e (0.97)	Inactive (0.94)	Active (0.65)	Inactive (0.90)	Active (0.57)	Inactiv e (0.85)

1,2,3-propanetriyl ester, indicatingpossible efflux transport and reduces accumulation of the ligands in intracellular spaces, limiting their efficacy. Glycidol stearate and Bicyclo[10.1.0] tridec-1-ene were the only predicted CYP inhibitors ensuring that most of the compounds possess no CYP inhibition and reduce the risk of drug-to-drug interactions (27). Most compounds had a bioavailability score of 0.55, while larger and lipophilic compounds had a score of 0.17, making compounds 3-hexen-2-one, 2-pentanethiol, and 9,12-octadecadienoic acid (Z, Z) as promising lead compounds.

3.2.3. *In-silico* Safety and Toxicology Assessment

In-silico toxicology assessment of the C. pepo bioactive compounds were evaluated based on their LD_{50} values (mg/kg), toxicity class, toxicological endpoints and systemic effects (Table 5). The compounds showed predicted LD_{50} values ranging from 810 mg/kg to 10,000 mg/kg, having toxicity classes 4 to 6 classified based on the Globally Harmonized System (GHS) (28).

Compounds of glycidol stearate and 9,12-Octadecadienoic acid (Z, Z)- were predicted to be under toxicity class 6 as they had the highest LD_{50} value of 10,000 mg/kg. All compounds were predicted to be not hepatotoxic with high confidence scores indicating low to nil liver toxicity. Three compounds, namely benzene, ethyl- (0.58), benzene, 1,2-dimethyl- (0.76) and bicyclo[10.1.0]tridec-1-ene (0.59) showed neurotoxic potential, while only hexadecenoicacid, 2-hydroxy-1,3-propanediyl ester was predicted as nephrotoxic, with absence of cardiotoxicity for all compounds. Aromaticity and fatty acid ester containing compounds dodecanoic acid, 1,2,3-propanetriyl ester, lauric acid derivative and glycidol stearate were predicted as active carcinogens and mutagens, making them unfit for oral drug usage (29). Despite all compounds being predicted as non-immunotoxin and non-cytotoxic, compound glycidol stearate showed systemic toxicity; compounds like 3-nonanone and 3-hexen-2-one showed overall safer profiles.

Based on the comprehensive evaluation, compound 9,12-Octadecadienoic acid (Z, Z)emerged as the top candidate due to its superior binding affinity, high oral bioavailability and least toxicity. Glycidol stearate and Bicyclo[10.1.0] tridec-1-ene ranked second-best due to their good binding affinity, comparatively safer toxicity profile and drug-likeness properties. Therefore, 9,12-Octadecadienoic acid (Z, Z) was selected as the potential candidate for molecular dynamic simulation to analyze the binding patterns and stability of the docked complex.

3.3. Molecular Dynamics Simulation Analysis

Using molecular dynamics, 9,12-Octadecadienoic acid (Z, Z)was simulated with the HER2 protein for a duration of 100

Vol. 19 (Supplementary Issue 4), Oct-Dec 2025, ISSN 0973-8916 (Print)., 2230-7303 (Online)
10.5530/ctbp.2025.4s.4

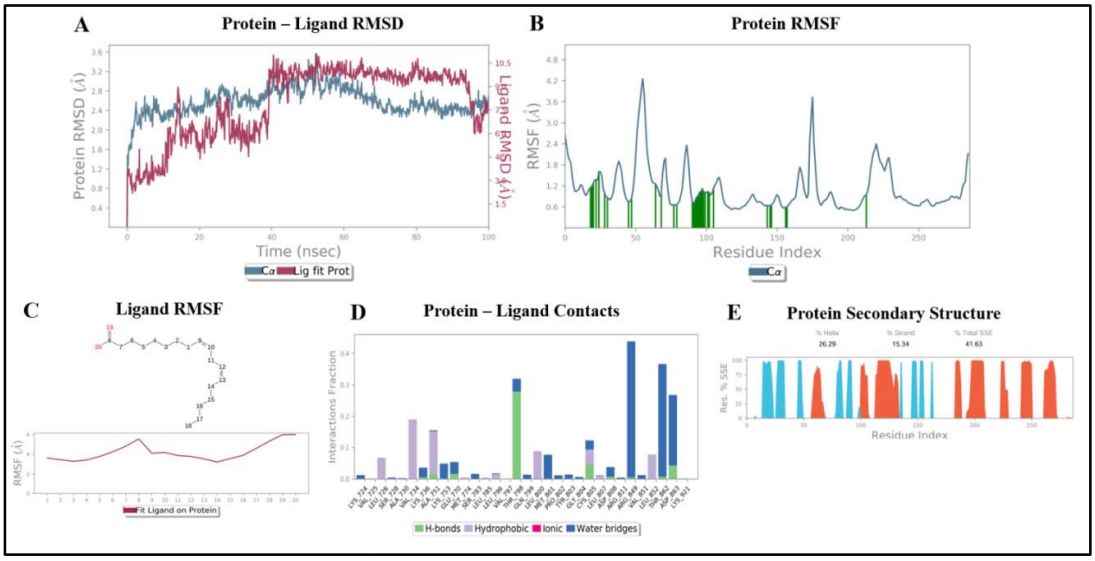

Fig. 3: Molecular Dynamics Simulation Analysis of the HER2-9,12-Octadecadienoic acid (Z, Z)-complex: (A) Protein-Ligand RMSD Analysis, (B) Flexibility Assessment of protein (C) Evaluation of Ligand Dynamics, (D) Interaction Profile of Protein Residues with the Ligand, and (E) Secondary Structure Analysis of Protein

nanoseconds. The simulated paths of Desmond were examined using MD trajectory analysis, the root-mean-square deviation (RMSD) and root-mean-square fluctuation (RMSF) to exhibit time-dependent variations in the protein and the ligand (Fig. 3).

RMSD analysis showed insights about the structural stability of the complex. The protein Cα atoms stabilized around 2.6 – 2.8 Å with an initial equilibration phase indicating that the protein maintained its structural integrity during the simulation (30). On the other hand, the ligand RMSD showed higher fluctuations before stabilizing around 3.2 Å with a sudden spike, followed by a stable phase after 40 ns, suggesting that it possesses moderate conformational flexibility within the protein's binding pocket. These fluctuations indicate the ligand's adaptive binding nature and making suitable interactions with key active site residues as time flows.

Protein RMSF plot showed that most residues especially the ones within the core binding site, had limited flexibility of <1.8 Å, indicating a stable conformation. However, visible and sharper fluctuations were observed at regions where loops and/or terminal regions are present (residue indices around 50, 170, and 210). These regions are generally more exposed to solvents and are inherently flexible; hence, they do not interfere with ligand binding (31, 32). Ligand RMSF profile depicts high fluctuations at atoms 8, 19 and 20, with the RMSF values reaching to 6.0 Å. Most of the central atoms showed moderate fluctuations of 3.5 - 4.5 Å, which is due to binding and dynamic rearrangement to stabilize interactions with the protein.

Interaction analysis revealed multiple key residues which modulate stable ligand binding, with major focus to residues THR798, ARG811 and ASP863, which formed hydrogen bonds and water bridges with the ligand. Hydrophobic residues such as VAL734 and VAL851 also contributed ligand binding through non-polar interactions, with all other residues involved in slightly less significant binding. Even though these

Vol. 19 (Supplementary Issue 4), Oct-Dec 2025, ISSN 0973-8916 (Print)., 2230-7303 (Online)
10.5530/ctbp.2025.4s.4

interactions are minimal, all interactions combined together support ligand's stable and dynamic binding, suitable for drug-like behaviour (33).

Table 6: MM-GBSA Binding Free Energy and Energy Component Analysis of the Protein-Ligand Complex in MD Simulation

Parameter	0 ns	100 ns
ΔGBind (MM-GBSA) (kcal/mol)	-94.24	-74.24
Ligand Strain Energy (kcal/mol)	5.24	1.33
Ligand Energy (kcal/mol)	-16.34	-28.4
Complex Energy (kcal/mol)	-8959.5	-9243.6
Receptor Energy (kcal/mol)	-8849	-9140.9
ΔGBind (NS) (kcal/mol)	-99.48	-75.57
Receptor Strain Energy (kcal/mol)	0	0
Ligand Efficiency (ΔGBind/Heavy Atom)	-4.71	-3.71

MM-GBSA analysis of the 100 ns MD simulation revealed a decrease of -94.24 to -74.24 kcal/mol in binding free energy. This indicates that binding affinity is slightly reduced,likely due to the conformational changes of the ligand (Table 6). In addition to this, ligand strain energy also reduced (from 5.24 to 1.33 kcal/mol), while ligand energy increased from -16.34 to -28.40 kcal/mol, making it favorable for improved ligand stabilization (34). Complex and receptor energies were also observed to become more negative, with a slight decrease in ligand efficiency and constant receptor strain energy, thereby confirming system is stabilized over time.

4. Conclusion:

The compounds identified from the aqueous extract of *Cucurbita pepo* seeds showed diverse chemical structures and pharmacological properties. These compounds, when assessed through molecular docking studies against the HER2 protein, revealed lipid-based esters such as 9,12-octadecadienoic acid (Z, Z) and lauric acid derivatives to show strong binding interactions with HER2's active site residues. ADMET scrutinization together with Lipinski's Rule of Five showed long-chain fatty acid esters and glycerides to hold promise, with compound 9,12-Octadecadienoic acid (Z, Z) emerging as the most promising candidate. Molecular dynamics simulations of the HER2 - 9,12-Octadecadienoic acid (Z, Z) complex over 100ns run confirmed stable binding, moderate decline in binding free energy, increased ligand and system stabilization. This optimal binding, favorable pharmacokinetics and low toxicity of 9,12-Octadecadienoic acid (Z, Z) warrants future experimental validation to confirm its usage in HER2-targeted cancer therapy.

References

1. Hoffe S, Balducci L. Cancer and age: general considerations. Clinics in geriatric medicine. 2012 Feb 1;28(1):1-8.
2. Sung H, Ferlay J, Siegel RL, Laversanne M, Soerjomataram I, Jemal A, Bray F. Global cancer statistics 2020: GLOBOCAN estimates of incidence and mortality worldwide for 36 cancers in 185 countries. CA: a cancer journal for clinicians. 2021 May;71(3):209-49.
3. De Groot PM, Wu CC, Carter BW, Munden RF. The epidemiology of lung cancer. Translational lung cancer research. 2018 Jun;7(3):220.
4. Skrutkowski M, Saucier A, Eades M, Swidzinski M, Ritchie J, Marchionni C. Impact of a pivot nurse in oncology on patients with lung or breast cancer: symptom distress, fatigue, quality of life, and use of healthcare resources. InOncology nursing forum 2008 Nov 1 (Vol. 35, No. 6, p. 948). Oncology Nursing Society.
5. Konat-Bąska K, Matkowski R, Błaszczyk J, Błaszczyk D, Staszek-Szewczyk U, Piłat-Norkowska N, Maciejczyk A. Does breast cancer increasingly affect younger women? International journal of environmental research and public health. 2020 Jul;17(13):4884.

6. Gupta SC, Kim JH, Prasad S, Aggarwal BB. Regulation of survival, proliferation, invasion, angiogenesis, and metastasis of tumor cells through modulation of inflammatory pathways by nutraceuticals. Cancer and Metastasis Reviews. 2010 Sep;29(3):405-34.
7. Wang T, Nelson RA, Bogardus A, Grannis Jr FW. Five-year lung cancer survival: which advanced stage nonsmall cell lung cancer patients attain long-term survival?. Cancer: Interdisciplinary International Journal of the American Cancer Society. 2010 Mar 15;116(6):1518-25.
8. Krishnamurti U, Silverman JF. HER2 in breast cancer: a review and update. Advances in anatomic pathology. 2014 Mar 1;21(2):100-7.
9. Mar N, Vredenburgh JJ, Wasser JS. Targeting HER2 in the treatment of non-small cell lung cancer. Lung Cancer. 2015 Mar 1;87(3):220-5.
10. Nitta H, Kelly BD, Allred C, Jewell S, Banks P, Dennis E, Grogan TM. The assessment of HER2 status in breast cancer: the past, the present, and the future. Pathology international. 2016 Jun;66(6):313-24.
11. Nicolò E, Boscolo Bielo L, Curigliano G, Tarantino P. The HER2-low revolution in breast oncology: steps forward and emerging challenges. Therapeutic Advances in Medical Oncology. 2023 Feb;15:17588359231152 842.
12. Priya S, Satheeshkumar PK. Natural products from plants: Recent developments in phytochemicals, phytopharmaceuticals, and plant-based neutraceuticals as anticancer agents. Functional and preservative properties of phytochemicals. 2020 Jan 1:145-63.
13. Dhiman AK, Sharma KD, Attri S. Functional constitutents and processing of pumpkin: A review. Journal of Food Science and Technology. 2009 May;46(5):411.
14. Kumar VA, Pushparani VP, Baskar G, Beevi SK, Rajarajan TP, Subashini S. Apoptosis inducing anti-proliferative activity of Citrullus lanatus seeds against A549 cell lines. South African Journal of Botany. 2024 Aug 1; 171:96-105.
15. Balachandran P, Parthasarathy V, Kumar TA. Isolation of compounds from Sargassum wightii by GCMS and the molecular docking against anti-inflammatory marker COX2. International letters of chemistry, physics and astronomy. 2016 Jan 1; 63:1-2.
16. Kondapuram SK, Sarvagalla S, Coumar MS. Docking-based virtual screening using PyRx Tool: autophagy target Vps34 as a case study. InMolecular docking for computer-aided drug design 2021 Jan 1 (pp. 463-477). Academic Press.
17. Aertgeerts K, Skene R, Yano J, Sang BC, Zou H, Snell G, Jennings A, Iwamoto K, Habuka N, Hirokawa A, Ishikawa T. Structural analysis of the mechanism of inhibition and allosteric activation of the kinase domain of HER2 protein. Journal of Biological Chemistry. 2011 May 27;286(21):18756-65.
18. Prabhavathi H, Dasegowda KR, Renukananda KH, Karunakar P, Lingaraju K, Raja Naika H. Molecular docking and dynamic simulation to identify potential phytocompound inhibitors for EGFR and HER2 as anti-breast cancer agents. Journal of Biomolecular Structure and Dynamics. 2022 Jun 21;40(10):4713-24.
19. Zadorozhnii PV, Kiselev VV, Kharchenko AV. In silico ADME profiling of salubrinal and its analogues. Future Pharmacology. 2022 Jun 16;2(2):160-97.
20. Ferreira LG, Dos Santos RN, Oliva G, Andricopulo AD. Molecular docking and structure-based drug design strategies. Molecules. 2015 Jul 22;20(7):13384-421.
21. Hildebrand PW, Rose AS, Tiemann JK. Bringing molecular dynamics simulation data into view. Trends in Biochemical Sciences. 2019 Nov 1;44(11):902-13.
22. Shivakumar D, Williams J, Wu Y, Damm W, Shelley J, Sherman W. Prediction of absolute solvation free energies using molecular dynamics free energy perturbation and the OPLS force field. Journal of chemical theory and computation. 2010 May 11;6(5):1509-19.

23. Bragin PE, Mineev KS, Bocharova OV, Volynsky PE, Bocharov EV, Arseniev AS. HER2 transmembrane domain dimerization coupled with self-association of membrane-embedded cytoplasmic juxtamembrane regions. Journal of molecular biology. 2016 Jan 16;428(1):52-61.
24. Radhakrishnan N, Prabhakaran VS, Wadaan MA, Baabbad A, Vinayagam R, Kang SG. STITCH, physicochemical, ADMET, and in silico analysis of selected Mikania constituents as anti-inflammatory agents. Processes. 2023 Jun 5;11(6):1722.
25. Vraka C. Predictive in vitro methods in experimental nuclear medicine: Blood Brain Barrier Penetration. 2017
26. Wu K, Kwon SH, Zhou X, Fuller C, Wang X, Vadgama J, Wu Y. Overcoming challenges in small-molecule drug bioavailability: A review of key factors and approaches. International Journal of Molecular Sciences. 2024 Dec 6;25(23):13121.
27. Carpenter M, Berry H, Pelletier AL. Clinically relevant drug-drug interactions in primary care. American family physician. 2019 May 1;99(9):558-64.
28. Banerjee P, Kemmler E, Dunkel M, Preissner R. ProTox 3.0: a webserver for the prediction of toxicity of chemicals. Nucleic Acids Research. 2024 Jul 5;52(W1):W513-20.
29. Ghosh S, Tripathi P, Talukdar P, Talapatra SN. In silico study by using ProTox-II webserver for oral acute toxicity, organ toxicity, immunotoxicity, genetic toxicity endpoints, nuclear receptor signalling and stress response pathways of synthetic pyrethroids. World Scientific News. 2019(132):35-51.
30. Hollingsworth SA, Dror RO. Molecular dynamics simulation for all. Neuron. 2018 Sep 19;99(6):1129-43.
31. Zhang G, Su Z. Inferences from structural comparison: flexibility, secondary structure wobble and sequence alignment optimization. BMC bioinformatics. 2012 Sep 11;13(Suppl 15):S12.
32. Ashraf N, Asari A, Yousaf N, Ahmad M, Ahmed M, Faisal A, Saleem M, Muddassar M. Combined 3D-QSAR, molecular docking and dynamics simulations studies to model and design TTK inhibitors. Frontiers in Chemistry. 2022 Nov 2;10:1003816.
33. Corradi V, Sejdiu BI, Mesa-Galloso H, Abdizadeh H, Noskov SY, Marrink SJ, Tieleman DP. Emerging diversity in lipid–protein interactions. Chemical reviews. 2019 Feb 13;119(9):5775-848.
34. Godschalk F, Genheden S, Söderhjelm P, Ryde U. Comparison of MM/GBSA calculations based on explicit and implicit solvent simulations. Physical Chemistry Chemical Physics. 2013;15(20):7731-9.